



## **Supplementary Information for**

Assembly and organization of the N-terminal region of mucin  
MUC5AC: Indications for structural and functional distinction from  
MUC5B

Jerome Carpenter\*, Yang Wang\*, Richa Gupta\*, Yuanli Li, Prashamsha Haridass, Durai B. Subramani, Boris Reidel, Lisa Morton, Caroline Ridley, Wanda K. O'Neal, MariePierre Buisine, Camille Ehre, David J. Thornton, and Mehmet Kesimer\*\*

Mehmet Kesimer

\*\*Email: [kesimer@med.unc.edu](mailto:kesimer@med.unc.edu)

**This PDF file includes:**

**Supplementary Figures S1 to S6**

## Supplementary Figures

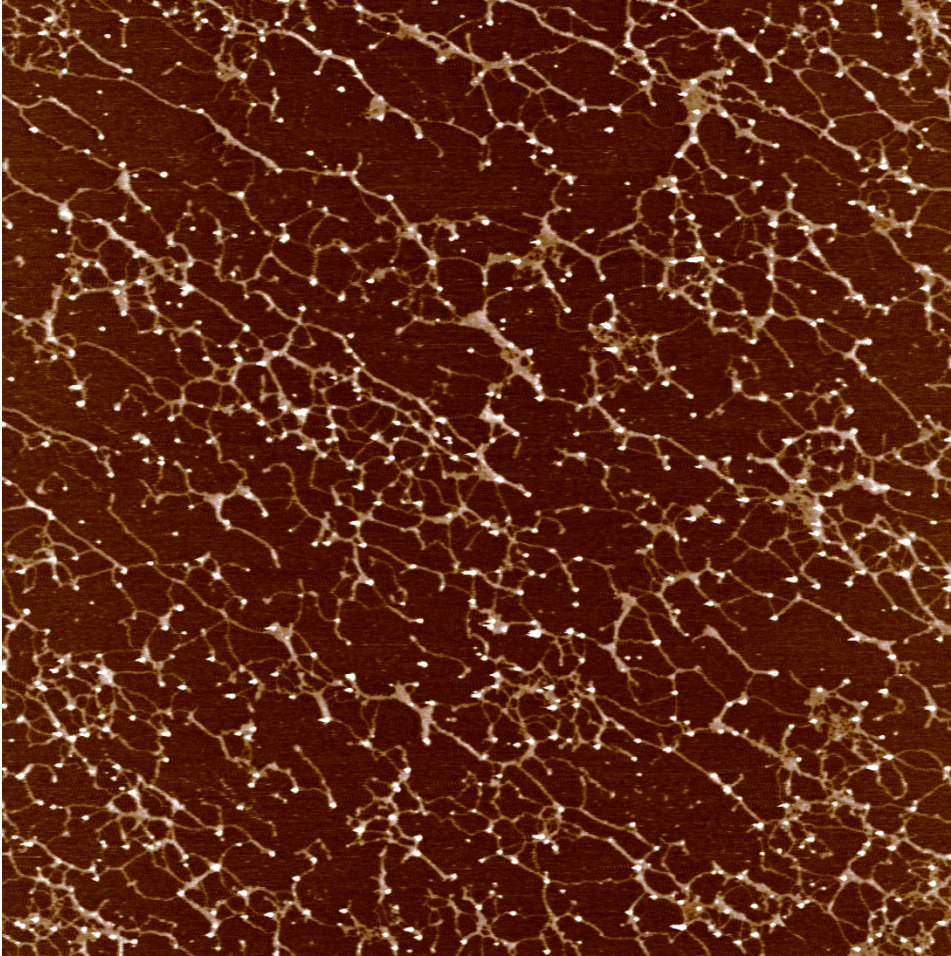


**Figure S1: AFM image of enriched MUC5AC and MUC5B standards mixed together.** AFM imaging of a MUC5AC preparation mixed with a MUC5B preparation reveals a similar macromolecular structure as observed in an AFM image of “wildtype” CALU3 preparation (Figure 2D), which had both MUC5AC and MUC5B present. Similar to that preparation, we observe a combination of the long linear filaments observed in isolated MUC5B and the highly branched and curled molecules observed in isolated MUC5AC. Scale bar is 1  $\mu\text{m}$ .

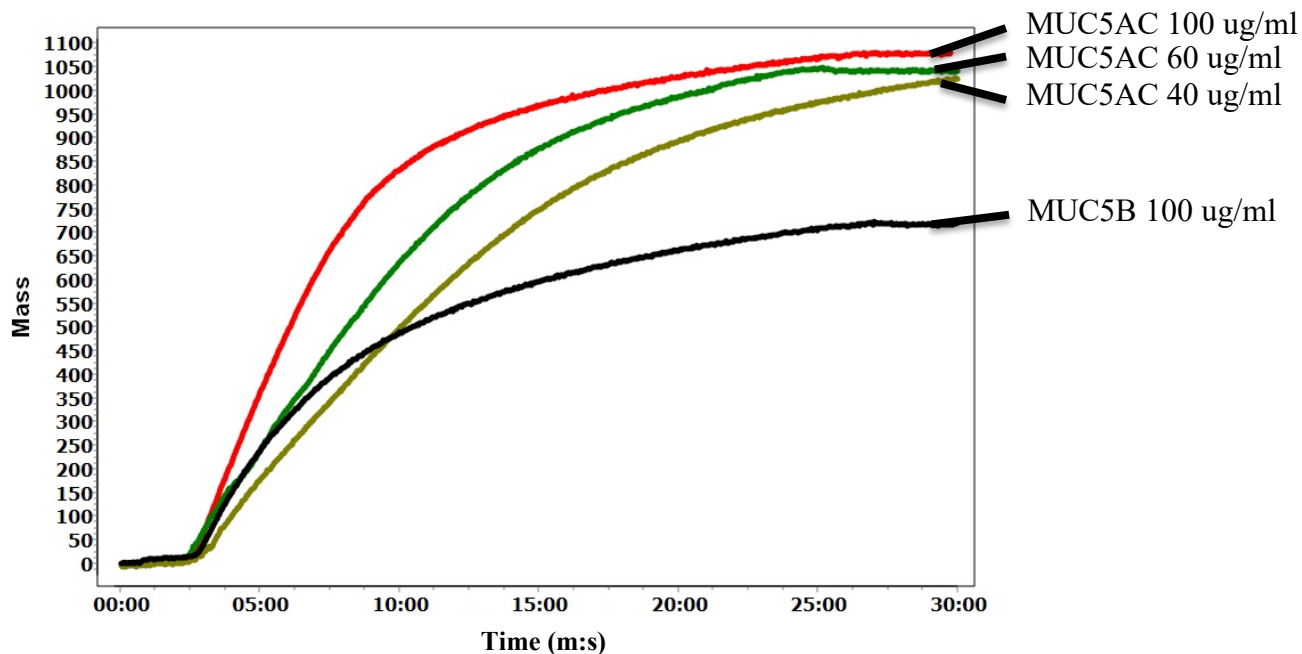


**Figure S2: Final mucin layer properties vs concentration in QCM-D experiments.**

Provided that there is enough material to form a complete mucin layer, the layer properties are independent of concentration. The plot above shows the calculated mass of several QCM-D experiments at various mucin concentrations. Ultimately, the three different concentrations of MUC5AC all plateau at approximately the same adsorbed mass regardless of the solution concentration. The concentration affects the time/slope required to reach the plateau. For comparison, MUC5B, which has different layer properties is shown.

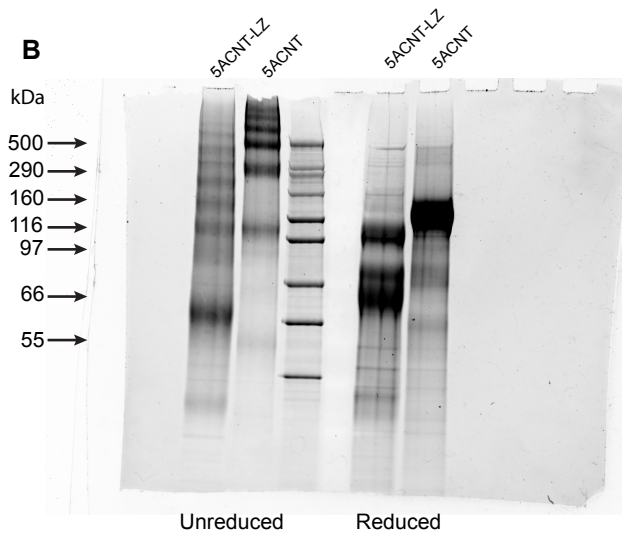
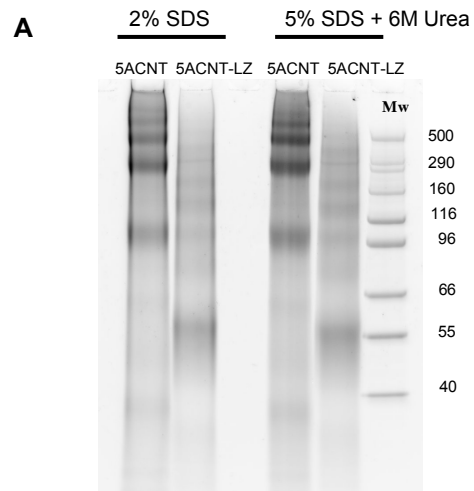


**Figure S3: Comparison of running conditions on 5ACNT and 5ACNT-LZ products on SDS-PAGE.** A) Sypro<sup>TM</sup> Ruby staining of SDS-PAGE of purified 5ACNT and 5ACNT-LZ proteins shows similar profile on 2% and 5% SDS in chaotropic agent Urea suggesting the oligomers are covalently bound with disulfide bonds. B) The entire gel from figure 5A, which was flipped and rearranged for clarity in the main text.

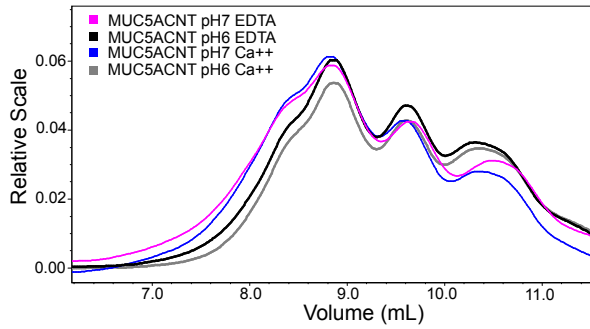


**Figure S4: SEC-MALLS analysis of the 5ACNT under different ionic conditions:** The 5ACNT protein product was equilibrated with buffers containing either 10 mM  $\text{Ca}^{++}$  or EDTA overnight at pH 6.0 or pH 7.4. A) The panel shows tREX refractometry traces of the resolving peaks of purified 5ACNT on a Superose 6 column under different pH and  $\text{Ca}^{++}$  conditions.

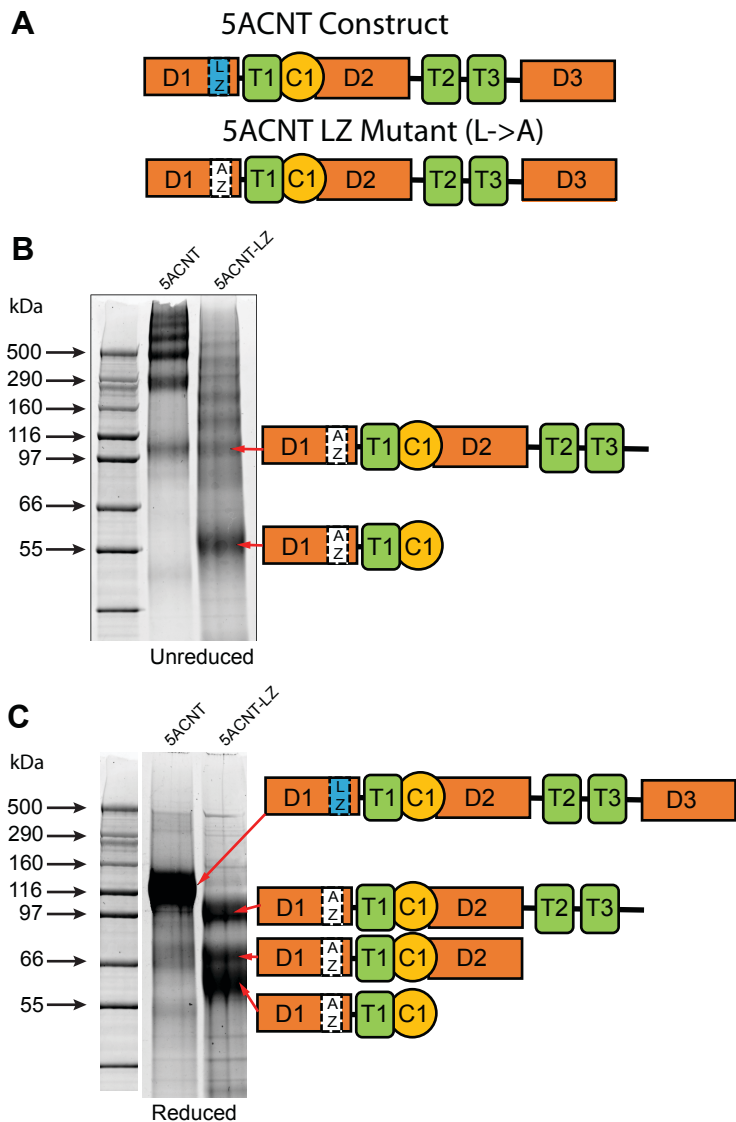


**Figure S5: Proteome coverage analyses of selected bands from the SDS\_PAGE: Bands were subjected to in-gel digestion and analyzed by mass spectrometry. A cartoon showing the domains of the 5ACNT construct (above) and the mutated 5ACNT-LZ construct, which has had the leucines of the leucine zipper replaced with alanines. We found that this construct did not produce the entire sequence and was missing the D3 domain. B) The 5ACNT protein shows all domains of the N-terminal region while the 5ACNT-LZ product shows no D3 domain. (C) After reduction, the 5ACNT-LZ construct collapses into three bands that contains different domains of the N-terminal region.**

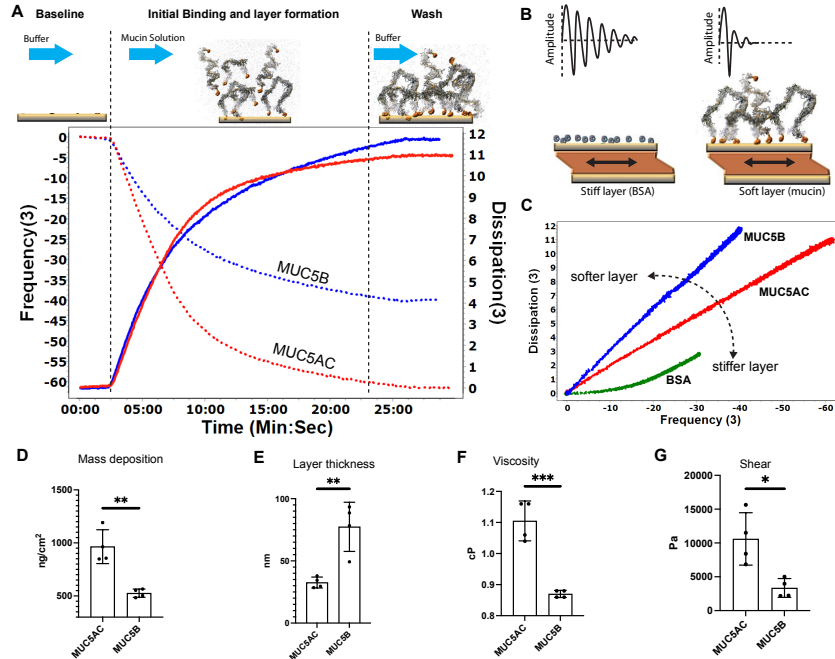


**Figure S6: Detailed legend for Fig 3:** (A) A cartoon depicting the time course of a QCM-D experiment with representative data for measurements with MUC5AC and MUC5B shown underneath (for comparison purposes two experiments are shown on the same axes, and only one overtone (F3/D3) is shown for simplicity). The experiments start with buffer flowing over an oscillating quartz sensor with a gold surface. During this phase the baseline resonance of the quartz crystal is recorded. Next a mucin solution is flowed over the gold surface, and mucins adsorb onto the gold surface, thus changing the resonant frequency. In general, as more mass adsorbs onto the surface, frequency (left y-axis, dashed lines) shifts more. Finally, buffer is flowed over the chip to wash it and establish a baseline of the adsorbed layer. For the same concentration (100ug/ml) of MUC5AC and MUC5B, MUC5AC causes a greater shift in frequency and shows a smaller dissipation (explained in panel B), which is shown by the solid lines and right axis. (B) Dissipation is the loss of energy in the system; the amplitude of the quartz crystal's oscillation is damped by the bound layer interacting with the buffer. The cartoon shows that for a layer that is tightly coupled (stiff, BSA as an example) to the crystal, there is a gradual decay in the amplitude. For a "softer" layer that has more interaction with the buffer (such as mucin), the damping occurs much faster. (C) A plot of dissipation vs frequency illustrates the different mechanical properties of materials. Stiffer materials have a smaller slope; their dissipation remains low as mass is added. Softer materials show a rapid increase in dissipation with increasing mass. MUC5AC is stiffer than MUC5B (BSA shown for comparison). (D) The Sauerbrey model calculated an absorbed MUC5AC layer of  $964 \pm \text{SD } 159 \text{ ng cm}^{-2}$  and MUC5B layer  $526 \pm \text{SD } 39 \text{ ng cm}^{-2}$ ,  $n=4$ . (E-G) Voigt modeling determined that (E) the MUC5AC layer was much thinner/denser ( $32.6 \text{ nm} \pm \text{SD } 4.4$ ,  $n=4$ ) compared to MUC5B layer ( $77.4 \text{ nm} \pm \text{SD } 19.7$ ,  $n=4$ ,  $p=0.0045$ ) and that (F) the viscosity ( $1.105 \text{ cP} \pm \text{SD } 0.06$ ,  $n=4$ ) and (G) shear elasticity ( $10600 \text{ Pa} \pm \text{SD } 3800$ ,  $n=4$ ) of MUC5AC layers were significantly higher compared to viscosity ( $0.87 \text{ cP} \pm \text{SD } 0.01$ ,  $n=4$ ) and shear elasticity ( $3300 \text{ Pa} \pm \text{SD } 1400$ ,  $n=4$ ) ( $P=0.02$ ) of the MUC5B layer. \* $P \leq 0.05$ , \*\* $P \leq 0.01$ , \*\*\* $P \leq 0.005$ .